JSR Publications

Available Online

J. Sci. Res. **4** (1), 99-107 (2012)

JOURNAL OF SCIENTIFIC RESEARCH

www.banglajol.info/index.php/JSR

Hydrothermal Novel Synthesis of Neck-structured Hyperthermia-suitable Magnetic (Fe_3O_4, γ-Fe_2O_3 and α-Fe_2O_3) Nanoparticles

M. S. Islam[a,c], J. Kurawaki[a*], Y. Kusumoto[a], M. Abdulla-Al-Mamun[a], M. Z. Bin Mukhlish[b]

[a]Department of Chemistry and Bioscience, Graduate School of Science and Engineering Kagoshima University, 1-21-35 Korimoto, Kagoshima 890-0065, Japan

[b]Department of Chemical Engineering & Polymer Science, Shahjalal University of Science and Technology, Sylhet, Bangladesh

[c]Department of Animal Husbandry and Veterinary Science, Faculty of Agriculture, University of Rajshahi,Rajshahi-6205, Bangladesh

Received 19 October 2011, accepted in revised form 28 November 2011

Abstract

Novel neck-structured Fe_3O_4, γ-Fe_2O_3 and α-Fe_2O_3 magnetic nanoparticles were successfully prepared by a modified hydrothermal method. Ferrous chloride tetrahydrate was solely used as a precursor for the novel nanomaterials. The X-ray diffractometric study revealed the purity of the nanomaterials thus synthesized. All of the products were characterized using a field-emission scanning electron microscope (FE-SEM) and a transmission electron microscope (TEM) for the particle size and morphology. Neck-structured particle morphology was observed for the first time in all of iron oxides with magnetic properties. The particle size observed was 50–60 nm. The synthesized nanomaterials showed excellent magnetization values when magnetic hysteresis loops were measured using a superconducting quantum interference device (SQUID). Moreover, the as-prepared magnetic nanoparticles suspensions showed significant temperature increments under an AC (alternating current) magnetic-field induction condition at room temperature which indicates the hyperthermia feasibility.

Keywords: Magnetic materials; Neck-structured; Hyperthermia; Heat dissipation.

doi:10.3329/jsr.v4i1.8727 J. Sci. Res. **4** (1), 99-107 (2012)

1. Introduction

The synthesis of nanostructured magnetic materials has become a particularly important area of research and is attracting a growing interest because of the potential applications such as materials in ferrofluids, advanced magnetic materials, catalysts, colored pigments, high-density magnetic recording media and medical diagnostics [1-6]. Iron oxides exist in

* *Corresponding author*: kurawaki@sci.kagoshima-u.ac.jp

nature in many forms in which magnetite (Fe_3O_4), maghemite (γ-Fe_2O_3) and hematite (α-Fe_2O_3) are probably the most common [7]. Hematite (α-Fe_2O_3) is the oldest iron oxide and is widespread in rocks and soils. It is the most stable iron oxide under ambient condition and has significant scientific and technological importance [8]. The stability and semiconductor (n-type) properties of α-Fe_2O_3 allow it to be used as a photocatalyst [9]. Currently the α-Fe_2O_3 photoelectrode has received considerable attention as a solar energy conversion material due to its excellent properties, such as a small band gap (2.1 eV), high resistivity to corrosion and low cost [10] and we already reported its cancer cell killing potentiality [11].

Magnetite and maghemite have attracted attention in biomedical applications because of their biocompatibility and low toxicity in the human body [12-15]. A major area of application has been the field of bio-assays where the magnetic properties have been exploited *in vitro* to manipulate magnetite nanoparticles with an external magnetic field [12, 16]. In an alternating magnetic field, induced currents are generated in metallic objects, and as a consequence, heat is generated in the metal. This phenomenon is greatly enhanced in metals showing collective magnetic behavior. Thus, when a magnetic fluid is exposed to an alternating magnetic field, the particles become powerful heat sources, destroying tumor cells since these cells are more sensitive to temperatures in excess of 41 °C than their normal counterparts [17]. The catalytic and other properties depend on the morphology, particle size and surface area. Besides, this preparation method plays a key role in determining the particle size and shape, size distribution, surface chemistry and therefore the applications of the material. In view of this, in the present study, we synthesized novel neck-structured Fe_3O_4 nanoparticles and transferred to γ-Fe_2O_3 and α-Fe_2O_3 by the modified hydrothermal method for the first time and observed hyperthermia capability.

2. Experimental

2.1. *Materials and methods*

Typical syntheses of magnetite (Fe_3O_4) nanoparticles were carried out in a hydrothermal system by modified reduction reactions between $FeCl_2$ and ethylene glycol and then the magnetite nanoparticles were oxidized into maghemite and hematite at 250 °C for 8 h in the presence of oxygen and at 500 °C for 3 h in the presence of Ar gas, respectively. In this experiment chemicals used were iron (II) chloride tetrahydrate ($FeCl_2$•4H2O, Wako Pure Chemical Industries Ltd., Japan), ethylene glycol (99.5%, Wako Pure Chemical Industries Ltd., Japan), polyethylene glycol (4000, Tokyo Kasei Kogyo Co. Ltd, Japan) and sodium acetate, anhydrous (NaAc, 98%, Nacalai Tesque, Japan). All chemicals were of analytical grade and were used without any further purification.

2.2. *Synthesis and formation of magnetic nanoparticles*

In this report, we synthesized neck-structured Fe_3O_4 nanoparticles by a modified hydrothermal method. Deng *et al.* prepared magnetic microspheres using $FeCl_3$•$6H_2O$ as a precursor and autoclaved the mixture at 200 °C for 8-72 h [18]. However, we used $FeCl_2$•$4H_2O$ as a precursor and the mixture was autoclaved at 190 °C for 5 h with air pressure 0.2 MPa to synthesize Fe_3O_4 magnetic nanoparticles. $FeCl_2$•$4H_2O$ (0.99 g, 5 mmol) was dissolved in ethylene glycol (40 mL) to form a clear solution, followed by the addition of NaAc (3.6 g) and polyethylene glycol (1.0 g). The mixture was stirred vigorously for 45 min until getting a clear solution and then sealed in a teflonlined stainless-steel autoclave (50 mL capacity). The autoclave was heated to and maintained at 190 °C for 5 h and allowed to cool to room temperature. After cooling, decantation was done by a permanent magnet to get the sedimented black products. The black products were washed several times with ethanol and dried at 70 °C for 3 h. Finally, we obtained 0.81 g of Fe_3O_4 nanoparticles. In hydrothermal synthesis, metal oxides particles are generally synthesized in aqueous solution of starting metal salts. In this case, oxygen of resulting oxide is derived from water as a reservoir but in our study $FeCl_2$•$4H_2O$ was the source of water during reaction. Moreover, polyethylene glycol (PEG) added in this reaction system acts as an oxidant, surfactant, and dispersing agent. This ultimately prevents the particle agglomeration and results in the formation of high surface area free-flowing Fe_2O_3. It is well known that Fe_3O_4 can be oxidized to γ-Fe_2O_3, which can be further transformed into α-Fe_2O_3 at higher temperatures [19]. However, magnetite (Fe_3O_4) is not very stable and is sensitive to oxidation. Magnetite is transformed into maghemite (γ-Fe_2O_3) in the presence of oxygen [20]. First, as-synthesized Fe_3O_4 was oxidized into γ-Fe_2O_3 at 250 °C for 8 h in the presence of oxygen and then γ-Fe_2O_3 was calcinated at 500 °C for 3 h in the presence of Ar gas to get α-Fe_2O_3.

3. Characterization

The general structure characterization, including size and crystal structure of the as-synthesized neck-structured Fe_3O_4, γ-Fe_2O_3 and α-Fe_2O_3 was performed for the samples without any size sorting. To further confirm the crystal structure and overall phase purity, the nanoparticles with different sizes were examined using a powder X-ray diffractometer (XRD, PANalytical Advance) with CuKα radiation and a Ni filter. The surface morphology and nanoparticles size were determined using a field-emission scanning electron microscope (FESEM, model Hitachi S-4100H). Further, the shape of the nanoplates was analyzed by transmission electron microscopy (TEM, JEOL JEM-3010 VII TEM) operating at 300 kV. Magnetic hysteresis loops were measured by a superconducting quantum interference device (SQUID, Quantum Design MPMS-5). Finally, AC magnetic-field induced heating capability of prepared nanoparticles was studied to examine the hyperthermia potentiality of the as-synthesized neck-structured

Fe_3O_4, γ-Fe_2O_3 and α-Fe_2O_3 nanoparticles by dispersing in distilled water as well as in a minimum essential medium (MEM) and temperature increment for the every dish was measured by a digital thermometer (Sato Keiryoki-250WP II-R).

4. Results and Discussion

4.1. *XRD analysis*

The crystal structures of the prepared neck-structured magnetic (magnetite, maghemite and hematite) nanoparticles were observed by the XRD measurement. Typical XRD patterns of Fe_3O_4, γ-Fe_2O_3 and α-Fe_2O_3 are shown in Fig.1. As shown in Fig. 1, all samples were found to be consistent with the expected diffraction pattern of the *fcc* FeO structures. No diffraction peaks from other crystalline forms were detected, which demonstrates that these Fe_3O_4, γ-Fe_2O_3 and α-Fe_2O_3 samples had high purity and crystallinity (JCPDS, PDF, File No. 01-071-6336, 00-039- 1346 and 01-085-0599, respectively). Fig. 1(a) is the XRD pattern of Fe_3O_4 nanoparticles assembly obtained after oven drying at 70 °C for 3 h. Fig. 1 (b) shows the XRD pattern of the red-brown materials, γ-Fe_2O_3 obtained after oxidation of Fe_3O_4 at 250 °C for 8 h in the presence of oxygen and Fig. 1 (c) shows the XRD pattern of the dark red-brown materials, α Fe_2O_3 obtained after 500 °C annealing of γ-Fe_2O_3 in Fig. 1 (b) under Ar gas for 3 h.

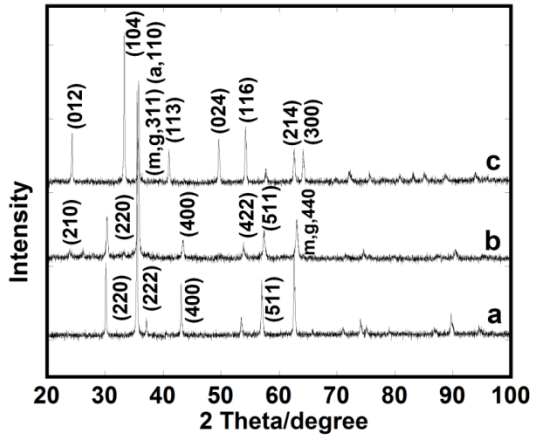

Fig. 1. X-ray diffraction patterns of (a) Fe_3O_4, (b) γ-Fe_2O_3 and (c) α-Fe_2O nanoparticles assembly obtained by hydrothermal method. Here m, g and a stands for Fe_3O_4, γ-Fe_2O_3 and α-Fe_2O_3, respectively.

In this paper, the structures of magnetic iron oxides were characterized by using X-ray diffraction analysis. Though magnetite and maghemite crystallizes under spinel structure, hematite does not. Thus, it is easy to differentiate between hematite and other magnetic iron oxides. However, it is very hard to identify magnetite and maghemite. But, in order to

confirm the three types of iron oxides nanoparticles prepared through this study, a comparative XRD analysis was done with commercial ones (see the supplemental information). Fig.1 shows that all XRD peak positions and relative intensities of our as-prepared nanomaterials match well with those of commercial.

4.2. *Shape analysis by FE-SEM and TEM*

Particles morphology of the samples was studied using FE-SEM. Fig. 2A (a), (b) and (c) represent the FE-SEM micrographs of Fe_3O_4, γ-Fe_2O_3 and α-Fe_2O_3, respectively. The nanoparticles size was roughly estimated to be about 60-70 nm from the SEM data, as shown in Fig. 2(A).

The samples were also characterized using TEM. Fig. 2B (a), (b) and (c) depict the TEM images of Fe_3O_4, γ-Fe_2O_3 and α-Fe_2O_3, respectively. The neck-structured morphology was observed by FE-SEM in all the samples. Such a type of unique morphology was observed for the first time for iron oxide with excellent magnetic properties.

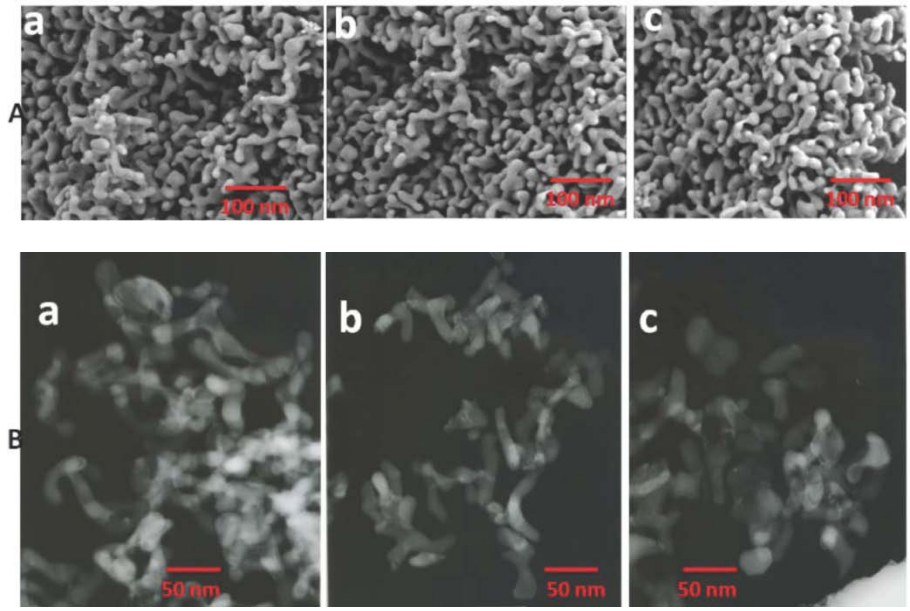

Fig. 2. (A) SEM and (B) TEM images of neck-structured magnetite, maghemite and hematite nanoparticles. Magnetite, maghemite and hematite nanoparticles are represented by (a), (b) and (c), respectively.

TEM images also clearly showed the nano-structural homogeneities and remarkably unique neck-structured morphology with average size of 50-60 nm. Although the neck-structure shaping mechanism is unclear, low temperature during autoclave, long time

oxidation and annealing may be responsible to the neck-structure formation. Further study is needed to clarify the mechanism.

Although the neck-structured property of γ-Fe_2O_3 and α-Fe_2O_3 nanoparticles with photocatalytic activity synthesized by combustion method have already been reported by Apte *et al*. [21] whereas we first time report the synthesis of neck-structured Fe_3O_4, γ-Fe_2O_3 and α-Fe_2O_3 nanoparticles with hyperthermia ability by simple hydrothermal decomposition.

4.3. *Magnetic properties of as-prepared nanomaterials*

Magnetic measurements on all kind nanoparticles indicate that the particles were superparamagnetic at room temperature, meaning that the thermal energy can overcome the anisotropy energy barrier of a single particle, and the net magnetization of the particle assemblies in the absence of an external field is zero. Fig. 3 shows the hysteresis loops of the as-prepared Fe_3O_4, γ-Fe_2O_3 and α-Fe_2O_3 nanoparticles, respectively, measured at room temperature.

Under a large external field, the magnetization of the particles aligns with the field direction and reaches its saturation value for Fe_3O_4, γ-Fe_2O_3 and α-Fe_2O_3 nanoparticles; we noticed that the saturation magnetization (*Ms*) values were 81, 63 and 1.6 emu/g, respectively, almost similar to the findings reported by Cornell *et al.* [7]. This is excellent evidence of the completion of the phase transfer of Fe_3O_4 to γ-Fe_2O_3 and α-Fe_2O_3.

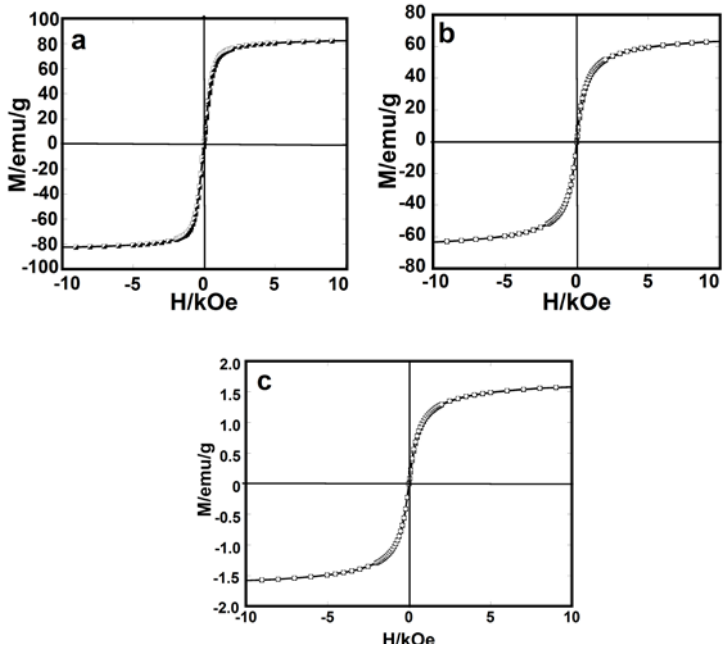

Fig. 3. Magnetic hysteresis loops of (a) Fe_3O_4, (b) γ-Fe_2O_3 and (c) α-Fe_2O_3 magnetic nanoparticles at room temperature.

4.4. *Heating capability*

Heat dissipation capability of as-prepared magnetic nanoparticles (Fe_3O_4, γ-Fe_2O_3 and α-Fe_2O_3) were evaluated by using an AC magnetic-field generator using maximum magnetic field intensity and a frequency of 5.0 kA/m and 560 KHz, respectively. The heat generated from all samples was evaluated by exposing 3 mg/mL magnetic nanoparticles suspension dispersed in distilled water and then their different doses like 0.2, 0.4, 0.6, 0.8 and 1.0 mL/5 mL MEM under the AC magnetic-field. The temperature rising of the as-prepared magnetic nanoparticles suspensions against the exposure time is shown in Fig. 4. The highest temperature was achieved as 48.7, 49.8 and 41.7 °C for Fe_3O_4, γ-Fe_2O_3 and α-Fe_2O_3, respectively, in 10 min exposure at a dose of 1.0 mL/5 mL MEM. These temperature increments of the as-prepared nanomaterials indicate the hyperthermia feasibility under an AC magnetic-field. Superparamagnetic nanoparticles when exposed to an alternating magnetic field can be used to heat tumor cells to 41- 45 °C, where damage for normal tissue is reversible while the tumor cells are irreversibly damaged [22]. The generation of heat by magnetic particles exposed to the alternating magnetic field depends very much on the magnetic particle characteristics such as saturation magnetization, particle size, magnetic field strength and frequency. When magnetic particles with diameters very much larger than the superparamagnetic limit are exposed to an AC magnetic-field, the heat is generated due to hysteresis loss. On the other hand, in the case of particles closer to superparamagnetic limit, they dissipate heat through Brownian or Néel relaxation depending on the alternating magnetic field frequency. Here again, the relaxation time depends on the particle diameter and when the particles are small and the relaxation time is comparable to the frequency, large amount of heat is generated [23].

It is noteworthy that due to some excellent advantages, ethylene glycol was used as a solvent instead of water in this experiment. The major use of ethylene glycol is as a medium for convective heat transfer, for example, in automobiles and liquid cooled computers. Ethylene glycol disrupts hydrogen bonding when dissolved in water. However, the boiling point for aqueous ethylene glycol increases monotonically with increasing ethylene glycol percentage. Both the literature [24, 25] and experimental evidences have led us to believe that ethylene glycol plays an important role in ferrite formation. Ethylene glycol is a strong reducing agent with a relatively high boiling point [25] and has been widely used in the polyol process to provide monodispersed fine metal or metal oxide nanoparticles. Moreover, possible advantages of the hydrothermal method over other types of crystal growth include the ability to create crystalline phases which are not stable at the melting point. Disadvantages of the method include the need of expensive autoclaves, and the impossibility of observing the crystal as it grows.

We believe that these hydrophilic and biocompatible neck-structured magnetic nanoparticles will have important applications not only in advanced magnetic materials and ferrofluids technology, but also in biomedical fields such as bimolecular separations, targeted drug delivery, cancer diagnosis and treatment as well as magnetic resonance imaging. Recently we reported the cytotoxicity effect of aqueous garlic extract (AGE) on

cancer cell [26] and further we are very interested to apply these nanomaterials in cancer (HeLa cell) treatment.

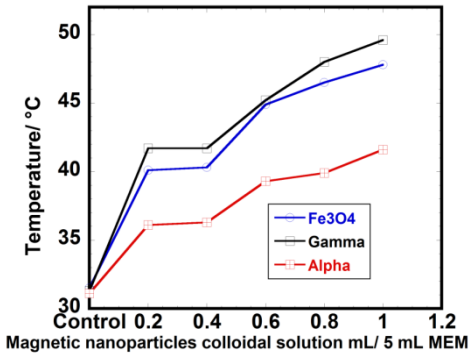

Fig.4. Heat dissipation capability of neck-structured magnetic nanoparticles synthesized by hydrothermal methods.

5. Conclusion

Nanosized neck-structured Fe_3O_4, γ-Fe_2O_3 and α-Fe_2O_3 magnetic materials have been prepared successfully from iron chloride tetrahydrate solely by the modified hydrothermal method. The FE-SEM and TEM studies revealed a unique necked structure with a particle size in the range of 50–60 nm. The synthesized nanomaterials also showed excellent magnetization values. Finally, the as-prepared magnetic nanoparticles suspensions showed significant temperature increments under an AC magnetic-field induction condition at room temperature, indicating the hyperthermia feasibility in cancer therapy.

Acknowledgement

The authors are very happy to acknowledge Associate Professor Yuji Horie and Hirotaka Manaka, Department of Electrical and Electronics Engineering, Graduate School of Science and Engineering, Kagoshima University, for the assembling of the AC magnetic-field induction instruments and analysis of hysteresis loops.

References

1. F. Caruso, M. Spasova, A. Susha, M. Giersig, and R. A. Caruso, Chem. Mater. **13,** 109 (2001). http://dx.doi.org/10.1021/cm001164h
2. T. Hyeon, S. S. Lee, J. Park, Y. Chung, and H. B. Na, J. Am. Chem. Soc. **123**, 12798 (2001). http://dx.doi.org/10.1021/ja016812s
3. Y. Xiong, Y. Xie, S. Chen, and Z. Li, Chem. Eur. J. **9**, 4991 (2003). http://dx.doi.org/10.1002/chem.200305118
4. K. Woo, H. J. Lee, J. Ahn, and Y. S. Park, Adv. Mater. **15**, 1761 (2003). http://dx.doi.org/10.1002/adma.200305561

5. Y. Wang, X. Teng, J. Wang, H. Yang, Nano. Lett. **3**, 789 (2003). http://dx.doi.org/10.1021/nl034211o
6. Y. F. Chong, K. L. Pey, A. T. S. Wee, M. O. Thompson, C. H. Tung, and A. See, Appl. Phys. Lett. **81**, 3768 (2002). http://dx.doi.org/10.1063/1.1521579
7. R .M. Cornell and U. Schwertmann, The Iron Oxides: Structure, Properties, Reactions, Occurrences and Uses, 2nd Edition (Wiley-VCH, Weinheim, 2003).
8. R. Dieckmann, Philos. Mag. A **68**, 725 (1993). http://dx.doi.org/10.1080/01418619308213994
9. H. H. Kung, Transition Metal Oxides: Surface Chemistry and Catalysis (Elsevier, New York, 1989).
10. T. Ohmori, H. Takahashi, H. Mametsuka, and E. Suzuki, Phys. Chem. Chem. Phys. **2**, 3519 (2000). http://dx.doi.org/10.1039/b003977m
11. M. S. Islam, Y. Kusumoto, M. Abdulla-Al-Mamun, and Y. Horie, Chem. Lett. **40**, 773 (2011). http://dx.doi.org/10.1246/cl.2011.773
12. P. Majewski and B. Thierry, Crit. Rev. Solid State Mater. Sci. **32**, 203 (2007). http://dx.doi.org/10.1080/10408430701776680
13. P. Tartaj, M. D. Morales, S. Veintemillas-Verdaguer, T. Gonzalez-Carreno, and C.J. Serna, J. Phys. D: Appl. Phys. **36**, R182 (2003). http://dx.doi.org/10.1088/0022-3727/36/13/202
14. J. S. Kim, T. J. Yoon, B. G. Kim, S. J. Park, H. W. Kim, K. H. Lee, S. B. Park, J. K. Lee, and M. H. Cho, Toxicol. Sci. **89**, 338 (2006). http://dx.doi.org/10.1093/toxsci/kfj027
15. P. Tartaj, M. P. Morales, T. Gonzalez-Carreno, S. Veintemillas-Verdaguer, and C. J. Serna, J. Mag. Mag. Mater. **290**, 28 (2005). http://dx.doi.org/10.1016/j.jmmm.2004.11.155
16. An-Hui Lu, E. L. Salabas, and F. Schüth, Angew. Chem. Int. Ed. **46**, 1222 (2007).
17. H. H. Yang, S. Q. Zhang, X. L. Chen, Z. X. Zhuang, J. G. Xu, and X. R. Wang, Anal. Chem. **76**, 1316 (2004). http://dx.doi.org/10.1021/ac034920m
18. H. Deng, X. Li, Q. Peng, X. Wang, J. Chen, and Y. Li, Angew. Chem. **117**, 2842 (2005). http://dx.doi.org/10.1002/ange.200462551
19. G. Bate, In Magnetic Oxides Part 2; D. J. Craik, Ed. (John Wiley & Sons, New York, 1975), pp 705-707.
20. L. Sophie, F. Delphine, P. Marc, R. Alain, R. Caroline, V. E. Luce, and N. M. Robert, Chem. Rev.**108**, 2064 **(**2008). http://dx.doi.org/10.1021/cr068445e
21. S. K. Apte, S. D. Naik, R. S. Sonawane, and B. B. Kale, J. Am. Ceram. Soc. **90**, 412 (2007). http://dx.doi.org/10.1111/j.1551-2916.2006.01424.x
22. T. Neuberger, B. Schopf, H. Hofmann, M. Hofmann, and B. von Rechenberg, J. Magn. Magn. Mater. **293**, 483 (2005). http://dx.doi.org/10.1016/j.jmmm.2005.01.064
23. J. P. Fortin, F. Gazeau, and C. Wilhelm, Eur Biophys J **37**, 223 (2008). http://dx.doi.org/10.1007/s00249-007-0197-4
24. Y. Lu, Y. Yin, B. T. Mayers, and Y. Xia, Nano Lett. **2,** 183 (2002). http://dx.doi.org/10.1021/nl015681q
25. Q. Peng, Y. Dong, and Y. Li, Angew. Chem. **115**, 3135 (2003). http://dx.doi.org/10.1002/ange.200250695
26. M. S. Islam**,** Y. Kusumoto, and M. Abdulla-Al- Mamun, J. Sci. Res. **3**, 375 (2011). doi:10.3329/jsr.v3i2.6557